Supporting Information: Molecular Simulation of Water and Hydration Effects in Different Environments: Challenges and Developments for DFTB Based Models

Puja Goyal,[a,†,⊥] Hu-jun Qian[a],[‡,¶] Stephan Irle,[§] Xiya Lu,[†] Daniel Roston,[†] Toshifumi Mori,[†,#] Marcus Elstner,[∥] and Qiang Cui[*,†]

Department of Chemistry and Theoretical Chemistry Institute, University of Wisconsin-Madison, 1101 University Avenue, Madison, WI 53706, Department of Chemistry, Graduate School of Science, Nagoya University, Nagoya, 464-8601, Japan, State Key Laboratory of Theoretical and Computational Chemistry, Institute of Theoretical Chemistry, Jilin University, Changchun 130021, China, Institute of Transformative Bio-Molecules (WPI-ITbM) & Department of Chemistry, Graduate School of Science, Nagoya University, Furo-cho, Chikusa-ku, Nagoya 464-8602, Japan, and Institute of Physical Chemistry, Karlsruhe Institute of Technology, Kaiserstr. 12, 76131 Karlsruhe, Germany

E-mail: cui@chem.wisc.edu

[a]Contributed equally

Neutral bulk water

Moments of water

The change in the dipole moment of water between gas phase and liquid phase reflects the treatment of polarizability by a simulation model. As shown in Fig. S1 and Table S1, while the change in the dipole moment of DFTB3 water between gas phase and liquid is somewhat underestimated compared to *ab initio* or DFT molecular dynamics (MD) simulations,[1] the average dipole moment in the liquid, ∼2.35 Debye, is very close to the dipole moment of classical water models like SPC/E and TIP3P;[1] a recent linear-scaling QM water model[2] also reported a liquid dipole moment around 2.5 Debye.

The importance of quadrupole moments has also been emphasized in the water literature.[1] As shown in Table S1, the gas phase Θ_2 for DFTB3/3OB(w) is substantially lower than the experimental value, although the solution value is in fact rather close to those from *ab initio* or DFT MD simulations. For reference, we have also listed the quadrupole moments for two popular non-polarizable water models, TIP3P and TIP4P/2005; both appear to substantially underestimate Θ_2 in the condensed phase.

*To whom correspondence should be addressed
†UW-Madison
‡Nagoya
¶Jilin University
§Nagoya & WPI-ITbM
‖KIT
⊥Current address: Department of Chemistry, University of Illinois at Urbana-Champaign, 505 South Mathews Avenue Urbana, IL 61801
#Current address: Institute for Molecular Science, Myodaiji, Okazaki, Aichi, 444-8585

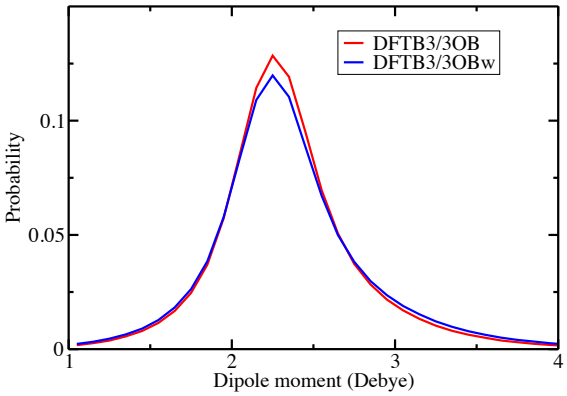

Figure S1: Dipole moment distribution in bulk water.

Table S1: Gas phase and liquid phase dipole (μ, in Debye) and quadrupole ($\Theta_{0,2}$, in Debye·Å)[a] moment of H_2O

	Exp.[b]	TIP3P	TIP4P/2005	DFTB3/3OB	DFTB3/3OBw
Gas phase μ	1.86	2.35	2.31	1.90	1.90
Liquid μ	∼2.5-3	2.35	2.31	2.35	2.36
Gas phase Θ_0 (Θ_0/μ)	0.11 (0.07)	0.23 (0.10)	0.18 (0.08)	-0.04 (-0.02)	-0.04 (-0.02)
Gas phase Θ_2 (Θ_2/μ)	2.57 (1.38)	1.72 (0.73)	2.30 (1.00)	1.61 (0.85)	1.61 (0.85)
Liquid phase Θ_0 (Θ_0/μ)	∼0.2 (∼0)	0.23 (0.10)	0.18 (0.08)	-0.35 (-0.15)	-0.37 (-0.16)
Liquid phase Θ_2 (Θ_2/μ)	∼3 (∼1.0)	1.72 (0.73)	2.30 (1.00)	2.87 (1.22)	2.88 (1.22)

[a] The quadrupole moments are computed as the following: 1. Orient each water molecule such that the O atom is at the origin, the bisector of the H-O-H angle is aligned along the positive Z-axis and the entire molecule lies in the Y-Z plane. 2. Calculate the quadrupole moment tensor using the new (after orientation) coordinates and the DFTB3 Mulliken charges. 3. Diagonalize the quadrupole moment tensor. 4. Relate the diagonal elements to Θ_0 and Θ_2 as defined in Eq. 2 of Ref.[1] [b] The gas phase experimental values are taken from Ref.;[3] for liquid phase, since no experimental values are available, values from CPMD or high-level QM/MM simulations cited in Ref.[1] are included for comparison.

Density and energetics of bulk water

It was observed previously that both DFTB2 and DFTB3 tend to overestimate the density of bulk materials, a trend most likely due to the underestimate of Pauli repulsion with the current DFTB methods.[4] Following this trend, NPT simulations with both DFTB3/3OB and

DFTB3/3OBw significantly overestimate the density of water ($\sim$1.3 g/cm^3 vs. $\sim$1.0 g/cm^3) at the ambient condition; note that the RMC optimization of the O-H repulsive potential is carried out with the NVT ensemble and experimental water density at ambient condition. On the other hand, the density obtained from NPT simulations using DFTB+[5] is rather sensitive to further adjustment of the O-H repulsive potential. In particular, to improve density, we find it effective to include a small additional linear term to the O-H repulsive potential, $\Delta V_{OH}^{rep} = A(1 - r/r_{cut})$, where r_{cut} is taken to be 7 Å, and A is adjusted to be 0.16 kcal/mol. Although this term has a negligible impact on the computed water structure from NVT simulations at ambient condition (see Fig. S2, compare 3OBw and 3OBwp; the latter includes the additional linear term in the O-H repulsive potential), it has a major impact on the computed density from NPT simulations. As shown in Fig. S3, the water density computed using the 3OBwp repulsive potential set, in fact, exhibits a density maximum in the expected temperature range. We caution, however, that this observation alone doesn't support DFTB3/3OBwp as a robust water model. What these exercises highlight is that the properties of bulk water are rather sensitive to the potential function and more systematic improvements of DFTB3 are required to lead to a physically robust model for water, even for situations near the ambient condition.

Another clear demonstration of limitations of the current DFTB3 formulation and the RMC scheme is that the improvement of bulk water structure in fact leads to deteriorated enthalpy of vaporization. As shown in Table S2, DFTB3/3OB NVT simulations at experimental water density underestimates ΔH_{vap} by about 2 kcal/mol, while the 3OBw parameter set further increases the error by another 2.4 kcal/mol. This is somewhat expected because the modification introduced by 3OBw effectively reduces each hydrogen bonding interaction by about 1 k_BT (see Fig. 3 in the main text), and a water in bulk on average forms four hydrogen bonds; for a water dimer in the gas phase, DFTB3/3OB predicts a binding energy of 4.6 kcal/mol, while 3OBw gives 4.0 kcal/mol. We note that the underestimate of ΔH_{vap} by the DFTB3 calculations is partly due to the fact that dispersion has not been in-

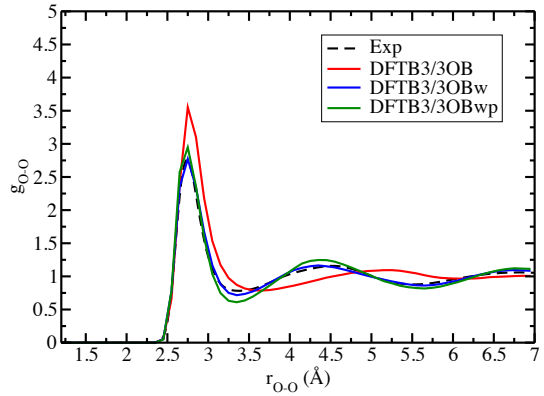

(a) g_{O-O}

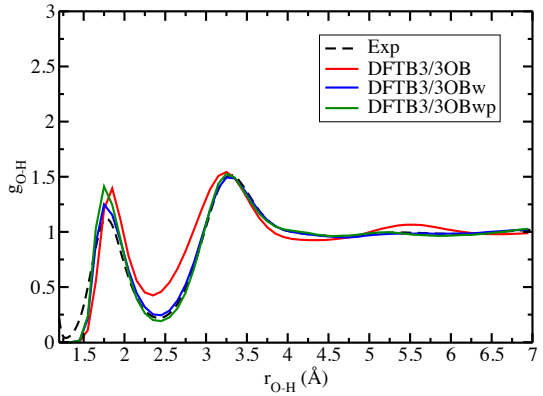

(b) g_{O-H}

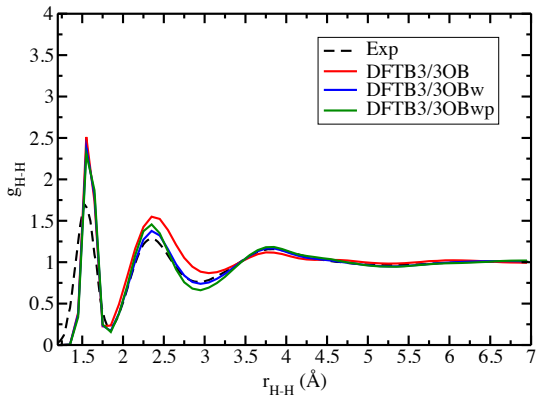

(c) g_{H-H}

Figure S2: Neutral water radial distribution functions (RDFs) from different DFTB3 simulations with NVT/NVE ensemble and experimental density at ambient condition. As discussed in the text, the 3OBwp adds a small linear term in the 3OBw O-H repulsive potential and gives good water density in NPT simulations for the ambient condition. Experimental data is from Ref.[6]

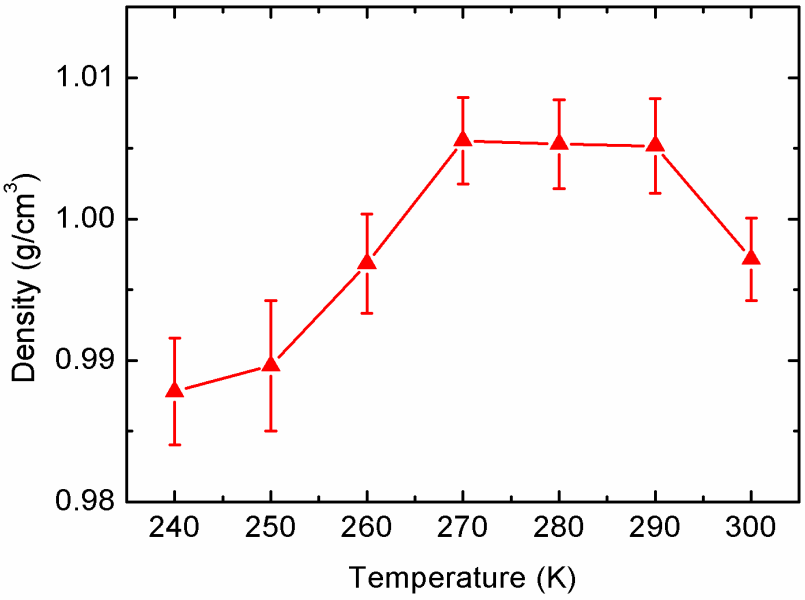

Figure S3: Temperature dependence of water density computed using NPT simulations (with 108 water molecules) and DFTB3/3OBwp. The original DFTB3/3OB and DFTB3/3OBw lead to substantially overestimated density at ambient condition (∼1.3 g/cm^3).

cluded; for ice Ih, two- and three-body dispersions have been estimated to contribute about 3 kcal/mol towards the cohesive energy per molecule.[7] Therefore, in the near future, it is important to explore bulk water simulations with the latest D3 dispersion model developed for DFTB3/3OB;[8] for DFTB3/MM applications with a modest number of QM water, however, it is unlikely that dispersion among QM atoms makes a significant contribution to the energetics. The consequence of the underestimated ΔH_{vap} for bulk water for DFTB3/MM applications needs to be carefully analyzed by, for example, computation of hydration free energies of hydrophobic and hydrophilic solutes; although water-water interactions are clearly underestimated, hydrogen bonding interactions among water are often persistent in the presence of solutes thus errors in the computed solution properties are expected to be less severe than that for ΔH_{vap}.

Table S2: Heat of vaporization, ΔH_{vap} (kcal/mol), for neutral bulk water from NVT simulations at experimental density at ambient condition

Exp.[a]	DFTB2[b]	DFTB2-γ^{hb}	DFTB3-diag[c]	DFTB3/ 3OB	DFTB3/ 3OBw
10.50	4.09±0.04	7.00±0.08	8.48±0.02	8.28±0.01	5.79±0.04

[a]Ref.[9] [b]Ref.[10] [c]Ref.[11]

Protonated water clusters, solvated proton and hydroxide

For the gas-phase protonated water dimer, $H^+(H_2O)_2$, Fig.S4 shows DFTB3/3OB barriers to be somewhat lower than those predicted by MP2/aug-cc-pVDZ. However, as we show in the main text and below, the "zero-temperature" Eigen-Zundel balance in larger protonated water-clusters like $H^+(H_2O)_6$ and $H^+(H_2O)_{22}$ as well as the Eigen/Zundel balance in finite-temperature MD simulations of $H^+(H_2O)_{21}$ and an excess proton in bulk water are satisfactory.

DFTB3/3OB shows significant improvement in the PES at r_{O-O}=2.4 Å compared to other SCC-DFTB variants (also see Fig. 1(a) in Ref. 11) in the sense that the energy does not rise as sharply as the proton moves away from the center between the two water molecules. This is expected to improve the shape of the proton transfer PMF in bulk water (see main text). Also, compared to the DFTB3-diag+gaus variant investigated in our previous work,[11] DFTB3/3OB shows the positions of the minima in the PES at r_{O-O}=2.54 Å and 2.6 Å in much better agreement with MP2/aug-cc-pVDZ results.

For other systems, additional results are summarized in the figures and tables below.

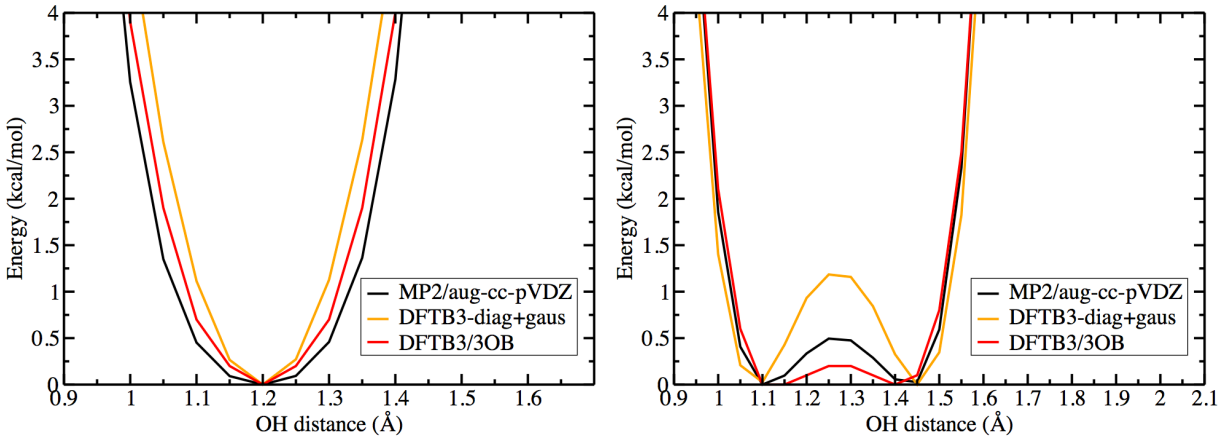

(a) r_{O-O}: 2.4 Å (b) r_{O-O}: 2.54 Å

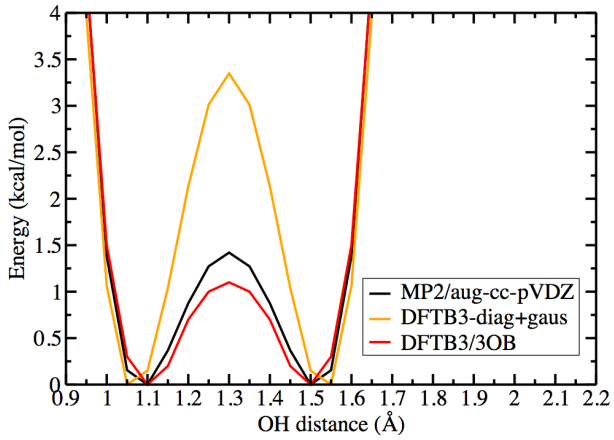

(c) r_{O-O}: 2.6 Å

Figure S4: Potential energy surface along r_{O-H} for fixed O-O distances of the protonated water dimer $H^+(H_2O)_2$.

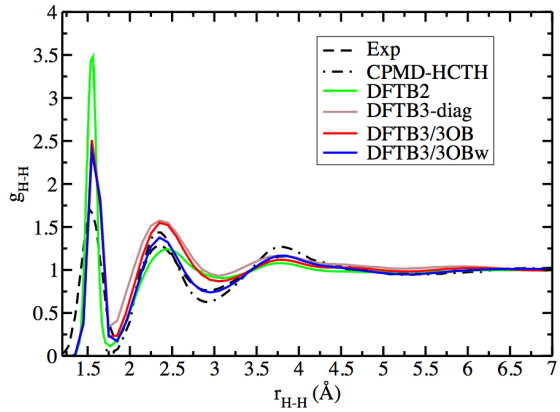

Figure S5: Comparison of H-H RDF calculated using various approaches and experimental data.[6] The CPMD and DFTB2 results are from Ref.[10] and the DFTB3-diag data is from Ref.[11]

Table S3: Energies relative to isomer VI (in kcal/mol) and Zundel/Eigen character of low-energy isomers of $H^+(H_2O)_6$ [a]

Isomer	MP2[b]			DFTB2[c]			DFTB3-diag+gaus[c]			DFTB3/3OB			DFTB3/3OBw		
I	0.47	(E)	(E)	2.06	(E-Z)	(E)	0.53	(E)	(E)	2.40	(E)	(E)	2.29	(E)	(E)
II	0.58	(E)	(E)	2.06	(E-Z)	(E)	0.53	(E)	(E)	1.12	(E)	(E)	2.30	(E)	(E)
III	0.09	(E)	(E)	2.06	(E-Z)	(E)	-0.48	(E)	(E)	1.11	(E)	(E)	2.30	(E)	(E)
IV	0.78	(E)	(E)	0.78	(Z)	(E-Z)	-0.03	(E)	(E)	1.67	(E)	(E)	2.66	(E)	(E)
V	0.00	(E)	(E)	1.34	(Z)	(E)	-0.40	(E)	(E)	-0.07	(E)	(E)	0.31	(E)	(E)
VI	0.00	(E)	(E)	0.00	(Z)	(E-Z)	0.00	(E)	(E)	0.00	(E)	(E)	0.00	(E)	(E)
VII	0.31	(E)	(E)	0.26	(Z)	(E-Z)	-0.47	(E)	(E)	-0.21	(E)	(E)	-0.19	(E)	(E)
VIII	0.56	(E-Z)	(E)	-0.79	(Z)	(Z)	0.03	(E)	(E)	0.07	(E-Z)	(E)	0.24	(E-Z)	(E)
IX	1.75	(Z)	(E-Z)	-1.30	(Z)	(Z)	0.09	(Z)	(Z)	-0.38	(Z)	(Z)	-1.22	(Z)	(Z)
X	1.39	(E)	(E)	1.11	(E-Z)	(E)	0.94	(E)	(E)	-0.12	(E)	(E)	-0.96	(E)	(E)
XI	4.01	(Z)	(E)	3.94	(Z)	(E)	3.28	(Z)	(Z)	4.36	(Z)	(E-Z)	5.79	(Z)	(Z)

[a]In the column for each method, the three sub-columns indicate the energy relative to isomer **VI**, Z/E/E-Z classification according to the criterion based on R_{OO} [12] and Z/E/E-Z classification according to the criterion based on δ.[10] [b]The MP2 relative energies are from Ref.[13] The MP2 results therein were obtained by single-point calculations with the aug-cc-PVTZ basis set at MP2/aug-cc-PVDZ optimized geometries. The Z/E/E-Z classification is based on the MP2/aug-cc-PVDZ geometries. [c]Ref. 11

Table S4: Summary of results for $H^+(H_2O)_6$. The errors are in the energies of 11 low-lying isomers relative to that of isomer VI (see Table S3) and are in kcal/mol. 'E' denotes Eigen. Def.1 denotes the criterion based on R_{OO}[12] while def.2 denotes the criterion based on δ[10]

	MP2[a]	DFTB2[b]	DFTB3 -diag+gaus[b]	DFTB3/ 3OB	DFTB3/ 3OBw
MAXE	0.0	-3.1	-1.7	-2.1	-3.0
RMSE	0.0	1.4	0.7	1.1	1.7
MUE	0.0	1.0	0.6	0.9	1.4
MSE	0.0	0.1	-0.5	0.0	0.3
# of E isomers (def.1)	8	0	9	8	8
# of E isomers (def.2)	10	6	9	9	9

[a]Ref. 13 [b]Ref. 11

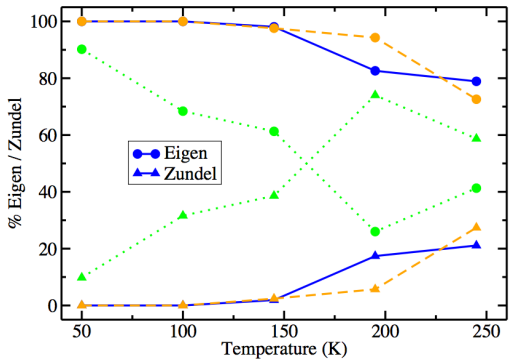

Figure S6: Population of Zundel and Eigen forms at different temperatures for the "magic" cluster $H^+(H_2O)_{21}$ from gas-phase MD simulations using DFTB3/3OBw (in blue), DFTB3-diag+gaus[11] (in orange) and DFTB2[11] (in green). CPMD-BLYP results from Singh et al.[14] agree well with those obtained with DFTB3/3OBw and DFTB3-diag+gaus.

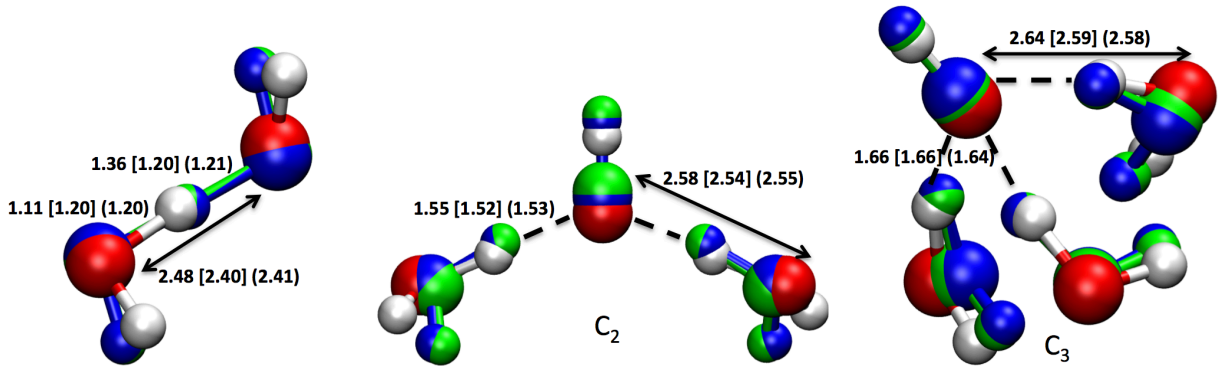

(a) n=1 (b) n=2 (c) n=3

Figure S7: Optimized structures of small hydroxide water clusters $(H_2O)_nOH^-$, n=1-3, with MP2/aug-cc-pVDZ (aug-cc-pVTZ for n=1) (colored by atom type), DFTB3/3OB (colored in blue) and DFTB3/3OBw (colored in green). Distances are displayed in the order: MP2, [DFTB3/3OB] and (DFTB3/3OBw). The starting structures are based on Ref. 15.

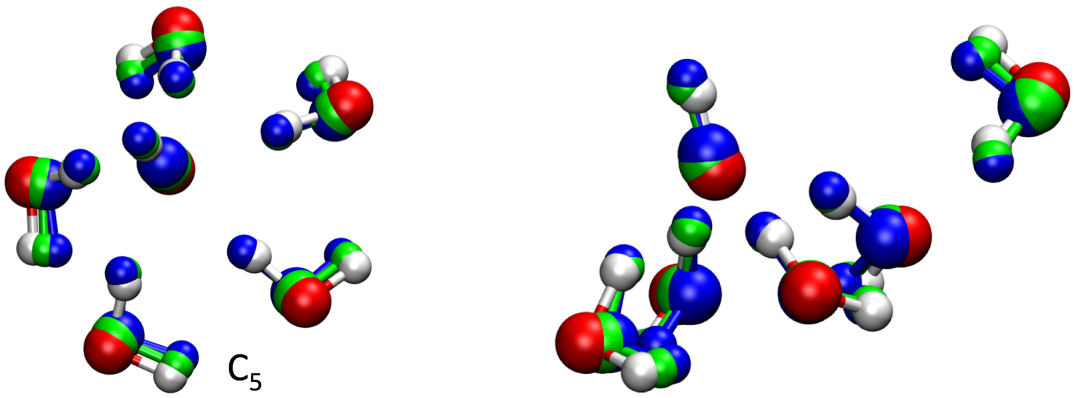

(a) Isomer I (b) Isomer II

Figure S8: Optimized structures of two isomers of $(H_2O)_5OH^-$ with MP2/aug-cc-pVDZ (colored by atom type), DFTB3/3OB (colored in blue) and DFTB3/3OBw (colored in green). The starting structures are based on Ref.[15]

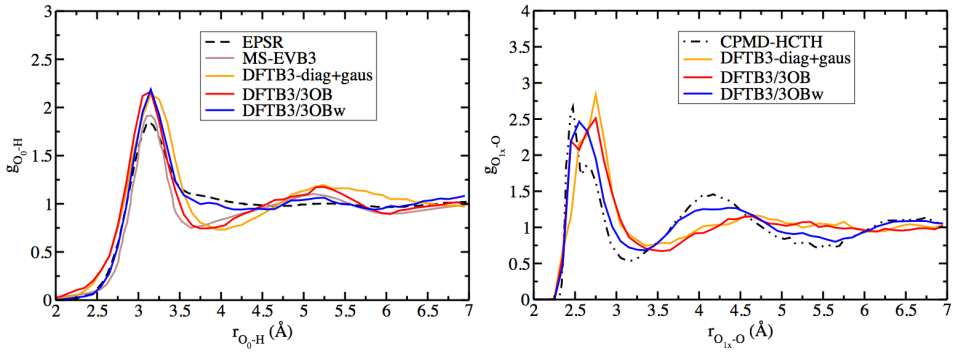

(a) g_{O_0-H} (b) $g_{O_{1x}-O}$

(c) $g_{O_{1yz}-O}$

Figure S9: RDFs associated with an excess proton in bulk water. The EPSR, CPMD-HCTH, MS-EVB3 and DFTB3-diag+gaus data are from Refs.,[16,17] Ref.,[10] Ref.[18] and Ref.[11] respectively.

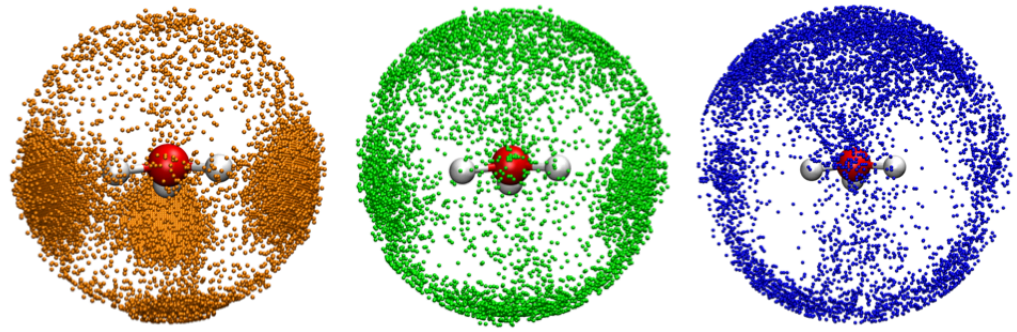

(a) DFTB3/3OB

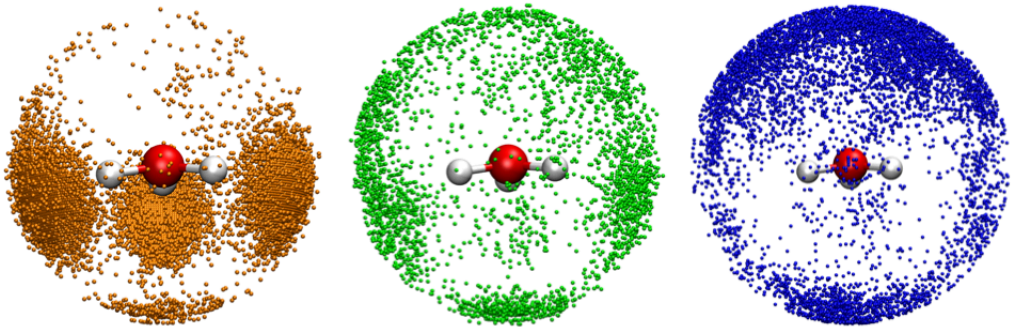

(b) DFTB3/3OBw

Figure S10: SDF of water O atoms3OBw around the hydronium O for a system comprised of an excess proton in bulk water. The different colors denote different O-O distance ranges. Only SDF > 3 is shown. Orange: 0.00 Å $< r_{O_0-O} <$ 2.75 Å; Green: 2.75 Å $< r_{O_0-O} <$ 3.05 Å; Blue: 3.05 Å $< r_{O_0-O} <$ 3.50 Å.

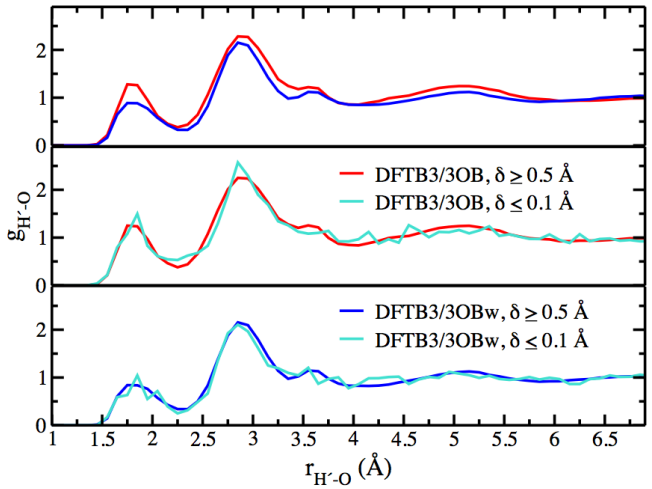

Figure S11: RDF of water O atoms around the hydroxide H, denoted H′. The top panel compares RDFs obtained with DFTB3/3OB (in red) and DFTB3/3OBw (in blue), using all simulation data. The middle and bottom panels compare the RDFs for configurations with large and small values of δ from DFTB3/3OB and DFTB3/3OBw respectively.

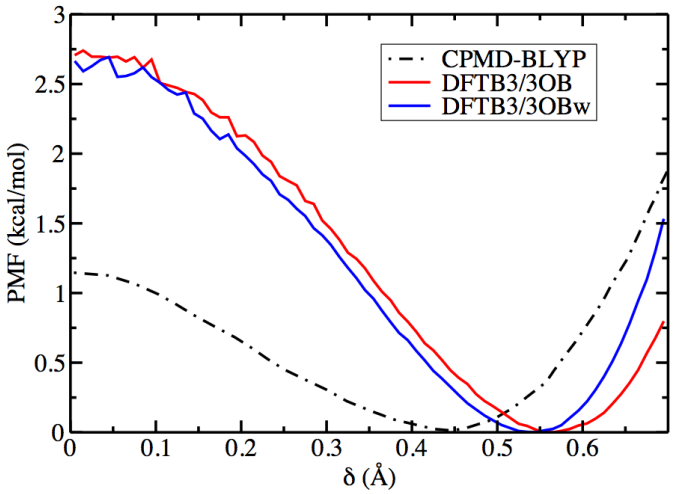

Figure S12: Potential of mean force for proton transfer to a hydroxide ion solvated in bulk water, using $\delta = \min|\ r_{O_0H} - r_{O_aH}\ |$ as the reaction coordinate (see main text for further explanation). The CPMD data is from Ref.[19]

QM/MM interactions

Table S5: Interaction energy (in kcal/mol) between the solute and nearby (∼6-13) water molecules at different levels

Solute	MM	QM/MM			Full QM			
		DFTB2 $1/R$	SCC-DFTBPR $1/R$ (KO)	DFTB3 $1/R$	DFTB2	SCC-DFTBPR	DFTB3	B3LYP[b]
Acetate	-81	-79	-84 (-61)	-85	-50	-65	-67	
	-84	-82	-87 (-74)	-86	-60	-75	-77	-67 (-80)
Methoxide	-102	-92	-98 (-75)	-97	-64	-80	-85	
	-107	-104	-111 (-90)	-110	-75	-94	-99	-85 (-95)

[a]For each solute, the first row uses ten clusters collected from the full MM window, and the second row uses ten clusters collected from SCC-DFTBPR/MM simulations that use the Klopman-Ohno (KO) form of QM-MM electrostatics. Due to limited sampling, there is substantial fluctuation in the interaction energies; the basic trends, however, are clear. The MM here is CHARMM22 force field, which uses a modified TIP3P model for water.
[b]The basis set is aug-cc-pVTZ. Values with parentheses also contain the D3 dispersion model of Grimme and co-workers.[8]

References

(1) Niu, S.; Tan, M.-L.; Ichiye, T. The large quadrupole of water molecules. *J. Chem. Phys.* **2006**, *124*, 074106.

(2) Han, J. B.; Mazack, M. J. M.; Zhang, P.; Truhlar, D. G.; Gao, J. L. Quantum mechanical force field for water with explicit electronic polarization. *J. Chem. Phys.* **2013**, *139*, 054503.

(3) Clough, S. A.; Beers, Y.; Klein, G. P.; Rothman, L. S. Dipole moment of water from Stark measurements of H2O, HDO and D2O. *J. Chem. Phys.* **1973**, *59*, 2254–2259.

(4) Gaus, M.; Cui, Q.; Elstner, M. Density Functional Tight Binding (DFTB): Application to organic and biological molecules. *WIREs Comput. Mol. Sci.* **2014**, *4*, 49–61.

(5) Aradi, B.; Hourahine, B.; Frauenheim, T. DFTB+, a sparse matrix-based implementation of the DFTB method. *J. Phys. Chem. A* **2007**, *111*, 5678–5684.

(6) Soper, A. K.; Benmore, C. J. Quantum differences between heavy and light water. *Phys. Rev. Lett.* **2008**, *101*, 065502.

(7) O. A. von Lilienfeld,; Tkatchenko, A. Two- and three-body interatomic dispersion energy contributions to binding in molecules and solids. *J. Chem. Phys.* **2010**, *132*, 234109.

(8) Risthaus, T.; Grimme, S. Benchmarking of London dispersion-accounting density functional theory methods on very large molecular complexes. *J. Chem. Theory Comput.* **2013**, *9*, 1580–1591.

(9) Marsh, K. N., Ed. *Recommended Reference Materials for the Realization of Physicochemical Properties*; Blackwell, 1987.

(10) Maupin, C.; Aradi, B.; Voth, G. The Self-Consistent Charge Density Functional Tight Binding method applied to liquid water and the hydrated excess proton: benchmark simulations. *J. Phys. Chem. B* **2010**, *114*, 6922–6931.

(11) Goyal, P.; Elstner, M.; Cui, Q. Application of the SCC-DFTB method to neutral and protonated water clusters and bulk water. *J. Phys. Chem. B* **2011**, *115*, 6790–6805.

(12) Choi, T.; Jordan, K. Application of the SCC-DFTB method to $H^+(H_2O)_6$, $H^+(H_2O)_{21}$, and $H^+(H_2O)_{22}$. *J. Phys. Chem. B* **2010**, *114*, 6932–6936.

(13) Kumar, R.; Christie, R.; Jordan, K. A modified MS-EVB force field for protonated water clusters. *J. Phys. Chem. B* **2009**, *113*, 4111–4118.

(14) Singh, N. J.; Park, M.; Min, S. K.; Suh, S. B.; Kim, K. S. Magic and antimagic protonated water clusters: Exotic structures with unusual dynamic effects. *Angew. Chem. Int. Ed.* **2006**, *45*, 3795–3800.

(15) Masamura, M. Ab initio MO study on the structures of OH- (H2O)(n) in the gas phase. *J. Mol. Struct. (Theochem)* **2000**, *498*, 87–91.

(16) Botti, A.; Bruni, F.; Imberti, S.; Ricci, M. A.; Soper, A. K. Ions in water: The microscopic structure of a concentrated HCl solution. *J. Chem. Phys.* **2004**, *121*, 7840–7848.

(17) Botti, A.; Bruni, F.; Ricci, M. A.; Soper, A. K. Eigen versus Zundel complexes in HCl-water mixtures. *J. Chem. Phys.* **2006**, *125*, 014508.

(18) Wu, Y.; Chen, H.; Wang, F.; Paesani, F.; Voth, G. An improved multistate empirical valence bond model for aqueous proton solvation and transport. *J. Phys. Chem. B* **2008**, *112*, 467–482.

(19) Choi, T. H.; Liang, R.; Maupin, C. M.; Voth, G. A. Application of the SCC-DFTB method to hydroxide water clusters and aqueous hydroxide solutions. *J. Phys. Chem. B* **2013**, *117*, 5165–5179.